Frequency-Domain Precoding for Single Carrier Frequency-Division Multiple Access

Mohamed Noune and Andrew Nix, University of Bristol

ABSTRACT

At present there is considerable interest in the use of single carrier frequency-division multiple access. This interest is justified by the inherent single carrier structure of the SC-FDMA scheme, which is more robust against phase noise and has a lower peak-to-average power ratio than orthogonal frequency-division multiple access. This consequently makes it more attractive for uplink transmission from low-cost devices with limited transmit power. SC-FDMA commonly makes use of frequency domain linear equalization in order to combat the frequency selectivity of the transmission channel. Frequency domain decision feedback equalization, composed of a frequency domain feed forward filter and a time domain feedback filter, outperforms LE due to its ability to cancel precursor echoes. Although these solutions suffer from error propagation, results show that DFE still offers a significant performance gain over conventional LE for uncoded SC-FDMA. In this article we show how precoding can be used on the uplink of the LTE standard to overcome the frequency selective nature of the radio channel. We propose a frequency domain implementation of Tomlinson-Harashima precoding and investigate the bit error rate and the PAPR performance for SC-FDMA using ZF and MMSE THP.

INTRODUCTION

The significant expansion seen in mobile and cellular technologies over the last two decades is a direct result of the increasing demand for high-data-rate transmissions over bandwidth and power limited wireless channels. This requirement for high data rates results in significant intersymbol interference (ISI) for single carrier systems, and therefore requires the use of robust coding and powerful signal processing techniques in order to overcome the time and frequency selective natures of the propagation channel. In recent years orthogonal frequency-division multiplexing (OFDM) has been proposed as an efficient high data rate solution for wireless applications. Particular examples include the physical layer of high-performance wireless local area networks (WLANs), such as the 802.11a/g/n, DVB-T/H, and 802.16 WiMAX standards. This trend has occurred since OFDM offers excellent performance in highly dispersive channels with low terminal complexity. For short-range devices, despite the high peak-to-average power ratio (PAPR) of the transmit OFDM signal [1], these solutions are now more common than their single carrier counterparts.

The Third Generation Partnership Project (3GPP) Long Term Evolution (LTE) radio access standard is based on shared channel access providing peak data rates of 75 Mb/s on the uplink and 300 Mb/s on the downlink. A working assumption in the LTE standard is the use of orthogonal frequency-division multiple access (OFDMA) on the downlink. This supports different carrier bandwidths (1.25–20 MHz) in both frequency-division duplex (FDD) and time-division duplex (TDD) modes [2]. OFDMA is an OFDM-based multiple access scheme [1] that provides each user with a unique fraction of the system bandwidth. OFDMA is highly suitable for broadband wireless access networks (particularly the downlink) since it combines scalability, multipath robustness, and multiple-input multiple-output (MIMO) compatibility [1]. OFDMA is sensitive to frequency offset and phase noise, and thus requires accurate frequency and phase synchronization. In addition, OFDMA is characterized by a high transmit PAPR, and for a given peak-power-limited amplifier this results in a lower mean transmit level. For these reasons, OFDMA is not well suited to the uplink transmission. Single carrier FDMA (SC-FDMA), also known as discrete Fourier transform (DFT) precoded OFDMA, has been proposed in the LTE standard for the uplink. In [3] the statistical PAPR characteristics are investigated for OFDM signals. Different techniques for PAPR reduction in OFDM signals are summarized in [3]. As demonstrated by these articles, PAPR reduction is motivated by a desire to increase the mean transmit power, improve the power amplifier efficiency, increase the data rate, and reduce the bit error rate (BER). This comes at the expense of cost, complexity, and efficiency. Ben Slimane, in [4], presents a novel linear PAPR reduction technique

 0163-6804/09/$25.00 © 2009 IEEE

for OFDM based on transmit precoding. Precoding, as its name implies, attempts to reduce the high PAPR of an OFDM system by multiplying the OFDM data by a precoding matrix prior to modulation. Design procedures for this precoding matrix are presented in [4]. It was shown that one design approach is equivalent to combining pulse shaping with decision feedback equalization (DFE) precoded OFDM.

The remainder of the article is organized as follows. In the next section an SC-FDMA transmission model is presented. We then describe the statistics of the PAPR for SC-FDMA compared to OFDMA. This is followed by a description of the different frequency domain equalization techniques that have been proposed for SC-FDMA. We then introduce the frequency domain Tomlinson-Harashima precoder (THP) for SC-FDMA, and present its performance together with a discussion of the issues that need to be addressed when designing the precoder. The final section concludes the article.

SC-FDMA

3GPP LTE is a driving force in the mobile communication industry. For high-data-rate wireless communications, multiuser (MU) transmission can be achieved through OFDMA and/or SC-FDMA. OFDMA has been chosen on the LTE downlink because of the spectral efficiency and robustness it offers in the presence of multipath propagation [1]. This immunity is a direct result of the narrowband transmissions that occur on each of the orthogonal subcarriers [5]. On the other hand, OFDMA waveforms are characterized by a high dynamic range, which results from the inverse DFT (IDFT) and translates to a high PAPR.

Signals with a high PAPR require the power amplifier to operate with a large backoff from the compression point. This effectively reduces both the mean power output level and the overall power efficiency. Different methods for PAPR reduction were proposed in [3] based on techniques dedicated to single-user (SU) OFDM. These include partial transmit sequence (PTS), selective mapping (SLM), and tone reservation (TR).

In [4] PAPR reduction was achieved through a transparent precoding scheme. The precoding example derived in this article is able to achieve PAPR reduction by combining pulse shaping with DFT precoded OFDMA. While the former bandlimits the signal, the latter reduces the DFT spread in the OFDMA modulator. This PAPR reduction technique is analogous to SC-FDMA. This is illustrated in Fig. 1. As can be seen, the only difference between SC-FDMA and OFDMA is the presence of a DFT and an IDFT block in the transmitter and receiver, respectively. Hence, SC-FDMA is also known as DFT precoded OFDMA. The principle of SC-FDMA signaling is presented in [2]. For each block of M data samples, the transmitter maps the corresponding M frequency components of this block, $\mathbf{X}$, resulting from an M-point DFT of the data samples, onto a set of M active subcarriers selected from a total of $N = QM$ subcarriers ($Q > 1$). The remaining $N - M$ subcarriers are inactive as they are used by other users on the uplink. In this article we consider distributed and localized

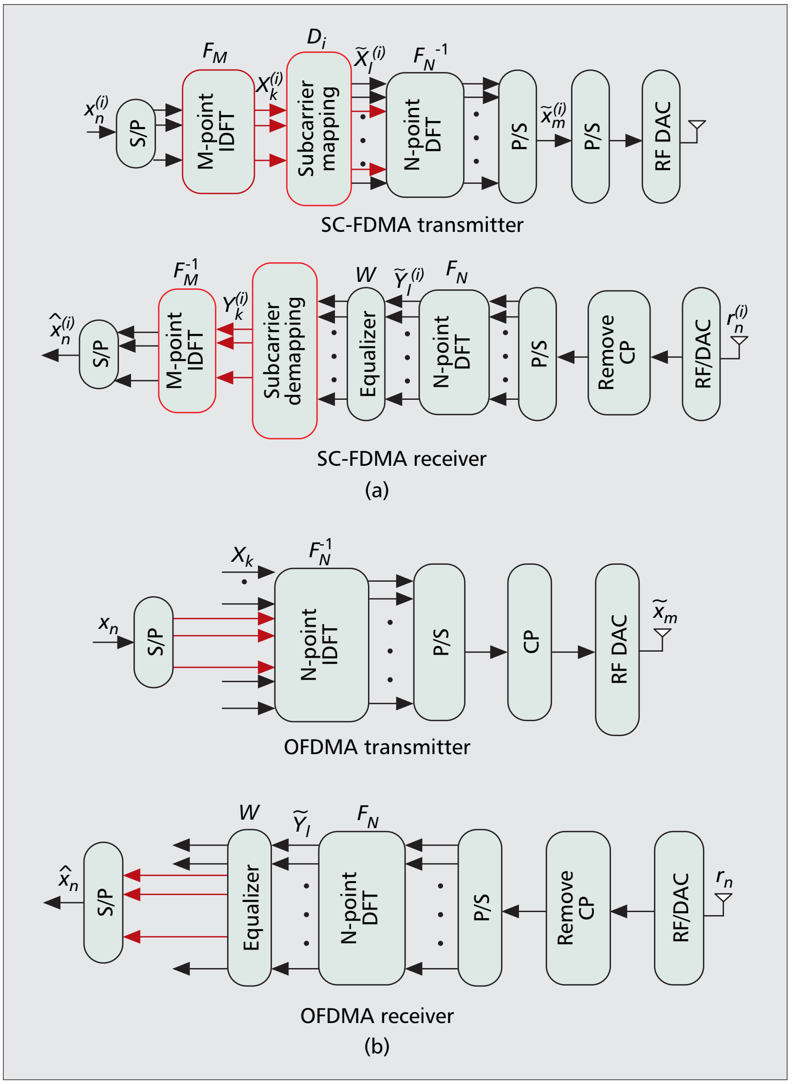

■ **Figure 1.** *Transceiver structure for SC-FDMA and OFDMA: a) SC-FDMA system diagram; b) OFDMA system diagram.*

SC-FDMA (D-FDMA and L-FDMA, respectively). Whereas D-FDMA was designed to better exploit frequency diversity even in an SU scenario, L-FDMA was designed to exploit the frequency selectivity of the channel at an MU level. The occupied bandwidth of an SC-FDMA system is confined to a fraction of the system bandwidth. The SC-FDMA transmitted signal can be represented by

$$\tilde{\mathbf{x}}^{(i)} = \mathbf{C}\mathbf{F}_N^{-1}\mathbf{D}_i\mathbf{F}_M\mathbf{x}^{(i)}, \tag{1}$$

where $\mathbf{F}_N^{-1}$ and $\mathbf{F}_M$ are the N-point IDFT and M-point DFT matrices, respectively. $\mathbf{D}_i$ denotes the subcarrier mapping for the ith user. $\mathbf{C}$ represents the CP insertion matrix.

The received signal $\mathbf{r}^{(i)}$ for the SC-FDMA system operating in a multipath fading channel corrupted by additive white Gaussian noise (AWGN), $\mathbf{w}^{(i)}$, with variance σ_n^2, is given by

$$\mathbf{r}^{(i)} = \mathbf{H}\tilde{\mathbf{x}}^{(i)} + \mathbf{w}^{(i)} = \mathbf{F}_N^{-1}\overline{\mathbf{H}}\mathbf{F}_N\tilde{\mathbf{x}}^{(i)} + \mathbf{w}^{(i)}, \tag{2}$$

where $\mathbf{H}$ is a circulant channel matrix, $\mathbf{w}$ is a column vector containing complex AWGN noise

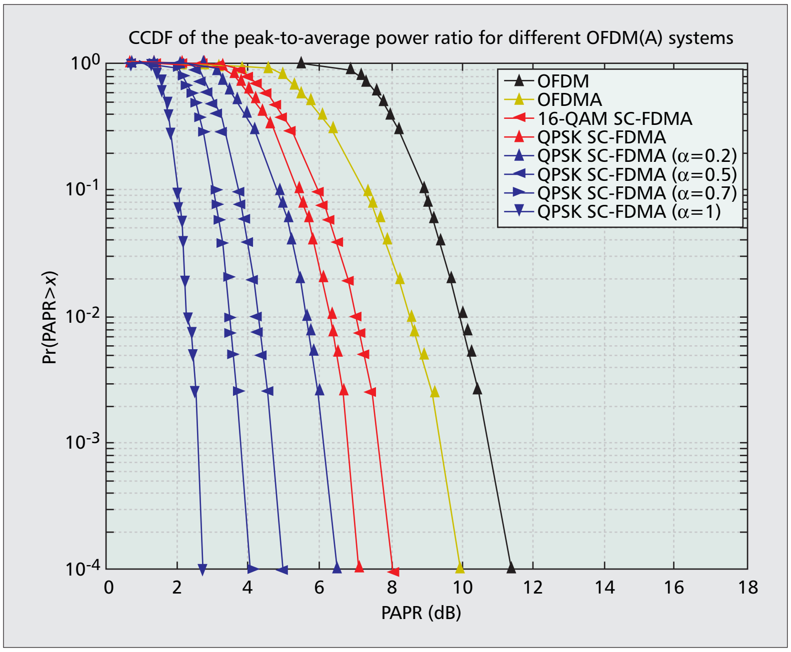

Figure 2. *PAPR characteristics of non-precoded SC-FDMA.*

samples, and $\overline{\mathbf{H}}$ is a diagonal matrix whose entries are generated from the N-point DFT of the channel impulse response.

PAPR Characteristics of SC-FDMA

Because of its single-carrier structure, SC-FDMA exhibits a lower PAPR than OFDM(A). For short-range transmissions, and in particular for battery powered devices, it is essential to transmit waveforms with low dynamic range. This ensures a low PAPR and therefore allows the power amplifier to operate in its linear range without excessive backoff. Figure 2 shows the complementary cumulative density function (CCDF) of the PAPR for OFDM, OFDMA, and SC-FDMA with quaternary phase shift keying (QPSK) and 16-quadrature amplitude modulation (QAM). For the case of SC-FDMA, the impact of pulse shaping is also illustrated. As a result, the oversampled L-FDMA and D-FDMA waveforms exhibit similar PAPR characteristics. The OFDM system was evaluated for different modulation schemes and numbers of subcarriers. For SC-FDMA and OFDMA the total number of subcarriers N was set to 512, and each user had access to 128 subcarriers with a spreading factor Q of 4. The CP length is $P = 64$. The subcarrier bandwidth is 15 kHz; hence, the duration of the SC-FDMA block is $\tau_s = 75$ μs. The PAPR was calculated for each OFDM(A)/SC-FDMA transmitted symbol. Overall, SC-FDMA offers a lower PAPR than OFDM and OFDMA. It is interesting to note that the PAPR of OFDM(A) is not dependent on the modulation scheme. This can be explained by the IDFT spreading of the modulated subcarrier symbols to generate the time domain waveform. The summation of multiple carriers, each of randomly modulated phase, clearly results in a Rayleigh envelope distribution irrespective of the original symbol constellation. OFDMA offers a lower PAPR than OFDM; however, this is still considerably higher than the equivalent SC-FDMA waveform. Unlike OFDM(A), the PAPR of the SC-FDMA waveform is sensitive to the choice of input constellation. This is due to the single carrier structure of SC-FDMA. The frequency domain subcarriers in SC-FDMA are modulated by the DFT spread time domain symbols. Hence, when the IDFT process is applied, the resulting time domain waveform is simply an upsampled version of the original symbol modulated sequence. Hence, the PAPR for QPSK modulated SC-FDMA is superior to that of 16-QAM modulated SC-FDMA.

Frequency domain pulse shaping is performed using a raised cosine filter. For QPSK modulation the effect of pulse shaping is shown for different values of raised cosine rolloff factor α. The power of the raised cosine filter is normalized to unity for all values of α. Since the raised cosine filter gives a smaller output peak power level with increasing α, we note that the PAPR reduces as α increases.

Subchannelization Gain

The use of subchannelization in FDMA permits more flexible use of the radio resources and supports mobile operation at longer ranges. Subchannelization adds a gain to the link budget and thus can be used to offset the losses associated with low antenna gains or in-building penetration. FDMA focuses the transmit power into a smaller group of carriers, thus increasing the power spectral density and providing a subchannelization gain. For instance, a 2 dB increase in the mean transmit power results in a 14 percent improvement in coverage for non-line-of-sight (NLOS) locations and a 19 percent increase in coverage for LOS locations. Furthermore, because of the use of subchannelization we can exploit small resource blocks to generate MU diversity through channel-dependent scheduling or generate a frequency diversity gain through frequency hopping (FH).

Channel Models and Assumptions

The 3GPP spatial channel model (SCM) was developed by the European Telecommunications Standards Institute (ETSI) 3GPP for MIMO simulations. It is based on a geometric ray model [2]. The introduction of multiple antennas in the 3G cellular standard requires detailed modeling of the spatial and temporal characteristics of the channel environment. The SCM defines three environments: suburban macro, urban macro, and urban micro. The resolvable path powers, delays, and angular properties for the base station and mobile handset are modeled as random variables defined through probability density functions (PDFs) and cross correlations. The SCM is able to simulate MIMO channels for systems including multiple cells/sectors, base stations (BSs), and mobile stations (MSs); it is not constrained to only a single link between a BS and a MS.

The SCM is designed for three of the most common cellular environments:

• **Suburban macrocell**: The suburban macrocell scenario describes rural/suburban areas characterized by residential buildings and structures. Vegetation and hills in the area are also assumed to be minor. The BS antenna position is well above the local clutter. As a result, the angle spread and delay spread are relatively small. The inter-BS distance is approximately 3 km.

- **Urban macrocell**: The urban macrocell scenario describes large cells in areas with urban buildings of moderate height. BS antennas are placed well above the rooftops of any buildings in the immediate vicinity. The inter-BS distance is approximately 3 km. This scenario assumes moderate to high angle spreads at the BS and large delay spreads.
- **Urban microcell**: In contrast to the above scenarios, the urban microcell scenario describes small urban cells with inter-BS distance less than 1 km. BS antennas are placed at the rooftop level and therefore produce large angle spreads at the BS, even though the delay spread is moderate.

Based on the 3GPP-SCM channel model, a number of different models for indoor, rural, urban, and suburban microcells can be defined. These include both LOS and NLOS channels. Large-scale fading (shadowing) and path loss parameters are also included. In this work we assume the use of urban LOS scenarios Range1 and Range2 B5b, as well as urban NLOS scenario C3.

EQUALIZATION FOR SC-FDMA

Because of its inherent single carrier structure, SC-FDMA can be considered an extension of SC-FDE [5], but with greater flexibility in resource allocation. SC-FDMA can be used with a range of single carrier equalization techniques to combat the frequency selective nature of the transmission channel. In fact, a common assumption in SC-FDMA is to use FDE. This includes frequency-domain linear equalization (LE), DFE, and the more recent turbo equalization:

- **FD-LE**: This is analogous to time domain LE. A zero-forcing (ZF)-based LE eliminates the ISI completely but introduces a severe degradation in the system's performance. This degradation is a result of the noise enhancement due to the gain inversion of deep spectral nulls. Superior performance can be achieved by using the minimum mean square error (MMSE) criterion, which minimizes the ISI distortion from the frequency selective fading channel and accounts for the additive noise.
- **FD-DFE**: Although FD-LE is simple, MMSE LE is not capable of fully flattening the frequency selective channel; this means that the equalized symbols experience some degree of residual ISI and noise. DFE offers superior performance to that of conventional LE, because of its ability to cancel residual ISI from the FDE without noise enhancement. DFE is considered for use on the uplink of 3GPP LTE to increase throughput and achieve more power-efficient transmission as demonstrated in [6]. Despite its superior performance relative to LE, the performance of DFEs are degraded due to error propagation when incorrect decisions are fed back through the device. As a result, the DFE suffers from a performance loss because of its inability to correct for long error bursts. This is especially noticeable when combined with forward error correcting (FEC) codes [6].

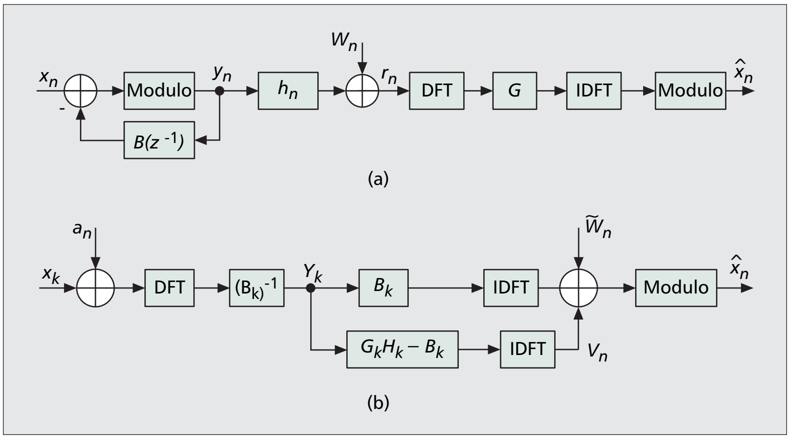

Figure 3. *Time domain and equivalent frequency domain structures of THP: a) THP precoder; b) THP equivalent structure.*

TRANSMIT PRECODING FOR SC-FDMA

DFEs are required to produce instantaneous decisions. When incorrect decisions are made, DFEs behave poorly due to error propagation. In order to overcome this shortcoming, alternative schemes have been proposed. These include block-based DFE, FDE with noise prediction, and THP [7, 8]. THP aims to obtain an ISI-free signal at the receiver by performing ISI cancellation prior to transmission (Fig. 3).

THP is an interesting way to account for the error propagation problem in a DFE since the feedback filter is implemented at the transmitter and is thus error-free. The operation of THP is presented in [7, 8], where the authors demonstrated that the multipath diversity of the wideband channel can be exploited at the transmitter through precoding.

THP based on the MMSE criterion has been shown to offer superior performance to that of MMSE DFE with perfect symbol knowledge in the feedback filter. Since perfect feedback is not possible in practice, THP tackles the error propagation problem in a DFE and offers a further improvement when coding is applied. In fact, because precoding does not suffer from error propagation, precoding has been combined with coded modulation schemes, such as Trellis precoding. Furthermore, THP, which was originally proposed to combat ISI for SU transmissions, was shown to be a suboptimal implementation of dirty paper coding and to achieve transmission at the full channel capacity.

There are several issues that need to be considered in the implementation of THP:

- **Channel state information feedback**: The transmitter requires full knowledge of the uplink channel in order to perform precoding. For TDD systems, as long as the time slot duration of the combined uplink and downlink transmission is less than the coherence time of the time-varying fading channel, the channel coefficients can be calculated at the BS during the uplink transmission and sent back to the resource unit. Thus, in this article we assume that channel estimation is performed at the BS, where the mean power of the wideband channel is normalized to unity and

As a result of precoding the dynamic range of the precoded waveform increases in the presence of deep channel fades. To overcome this problem THP can be implemented with a modulo operator.

the channel information is sent back to the mobile unit. This means that transmit precoding cannot compensate for fast fluctuations in the channel's mean power. In other words, precoding is only concerned with flattening the wideband channel and does not provide power control.

- **Maximum transmit power**: As a result of precoding, the mean transmit power per SC-FDMA symbol increases or decreases as a result of the magnitude fluctuations of the precoder's weights. Since the transmit power per symbol is constrained and fixed for transmission blocks, the mean transmit power should be constrained to the case observed per symbol without precoding.
- **Dynamic range**: As a result of precoding, the dynamic range of the precoded waveform increases in the presence of deep channel fades. To overcome this problem THP can be implemented with a modulo operator.

IMPLEMENTATION OF THP

We consider THP combined with SC-FDE for uplink SC-FDMA. The operation of THP is tightly connected to the modulated signal constellation. The implementation of THP in the context of SC-FDMA becomes deficient since the SC-FDMA signal does not have a distinct constellation in the time domain due to oversampling since only 1 in Q, and 1 in Q', samples fall on the transmit constellation for L-FDMA and D-FDMA, respectively. This means that SC-FDMA cannot benefit from time domain implementation of THP. In addition, due to the time domain implementation of the THP precoder, as the delay spread of the channel increases the implementation of the precoder requires greater computational complexity. For these reasons, we now derive a realizable and effective frequency domain implementation of the THP precoder. The precoder's coefficients are denoted b_k with $1 \leq k \leq L$, and L represents the length of the precoder's filter. The precoder's coefficients are derived as demonstrated in [9]. If the precoder's input is the SC-FDMA modulated signal after CP insertion, $\tilde{\mathbf{x}}$, by ignoring the modulo device the precoder's output is given by

$$y_n = \tilde{x}_n - \sum_{m=1}^{L} b_m y_{n-m}. \tag{3}$$

Since the precoder's filtering can be expressed as the cyclic convolution between the precoder's input and the precoder's impulse response, by taking the N-point DFT of both sides of this equation, the precoder's time domain filtering can be implemented as a frequency domain point-by-point multiplication between the output of the subcarrier mapping and the precoder's frequency response. The frequency domain implementation of the THP is

$$X_k = \left(1 + \sum_{n=1}^{L} b_n e^{-j2\pi\frac{kn}{M}}\right) Y_k = B_k Y_k, \tag{4}$$

which leads to $Y_k = B_k^{-1} X_k$, where X_k and Y_k denote the frequency response of the precoder's input and output, respectively. The implementation of the transmit precoder can therefore be moved from the time domain to the frequency domain. This reduces the ML multiplications and ML additions performed in the time domain implementation of the precoder to only M multiplications in the frequency domain, which translates to reduced complexity.

TRANSMIT POWER NORMALIZATION

The weights of the precoder must be power constrained. For each precoded SC-FDMA symbol, the mean transmit power is given by

$$\gamma^2 = \frac{1}{M} \sum_{k \in \Psi_i} \left| B_k^{-1} \tilde{X}_k \right|^2 = \sigma_s^2 \frac{1}{M} \sum_{k \in \Psi_i} \left| B_k^{-1} \right|^2, \tag{5}$$

where Ψ_i denotes the set of subcarriers occupied by user i.

In order to normalize the transmit power to the case without precoding, the precoder's output is divided by γ. This power normalization at the transmitter results in a gain mismatch between the feedback and feedforward filter at the output of the receiver. In order to compensate for gain mismatch between the transmitter and receiver, the output of the receiver has to be multiplied by γ. Since we assume that the transmitter and receiver are perfectly synchronous, and the multipath channel is static and perfectly known at both sides of the link, the receiver can compute γ as shown in Eq. 5.

PAPR CHARACTERISTICS AND ITS IMPACT ON TRANSMIT POWER

Figure 4a shows the CCDF of the PAPR for the ZF and MMSE THP waveforms for different values of M, calculated for each SC-FDMA symbol. For each precoded SC-FDMA symbol the PAPR was calculated as the ratio of the maximum transmit power to the mean transmit power:

$$PAPR = \frac{\max\left(\left|\tilde{x}_n\right|^2\right)}{\mathrm{mean}\left(\left|\tilde{x}_n\right|^2\right)}. \tag{6}$$

As can be seen, the PAPR of the ZF-THP is higher than the PAPR of the MMSE-THP for all M. This is a result of the high dynamic range of the magnitudes of the ZF-THP compared to MMSE-THP. In addition, the PAPR of both schemes reduce as the number of active subcarriers per user reduces. Since SC-FDMA can be seen as DFT precoded OFDMA, smaller DFT sizes (smaller M) offer lower DFT spreads in the OFDMA modulator; hence the reduction in the PAPR of the precoded SC-FDMA waveform. This reduction in the PAPR allows an increase in the mean power, which translates to improved coverage. For example, the 99 percent PAPR level (the PAPR level χ that satisfies Pr(PAPR $> \chi$) = 0.01) for $Q = 4$ offers an improvement of 1 dB over $Q = 2$, and an improvement of almost 2 dB over $Q = 1$ for both the ZF and MMSE THP. In addition to the subchannelization gain mentioned earlier, a further improvement in the mean transmit power density is seen as Q increases (i.e., smaller M).

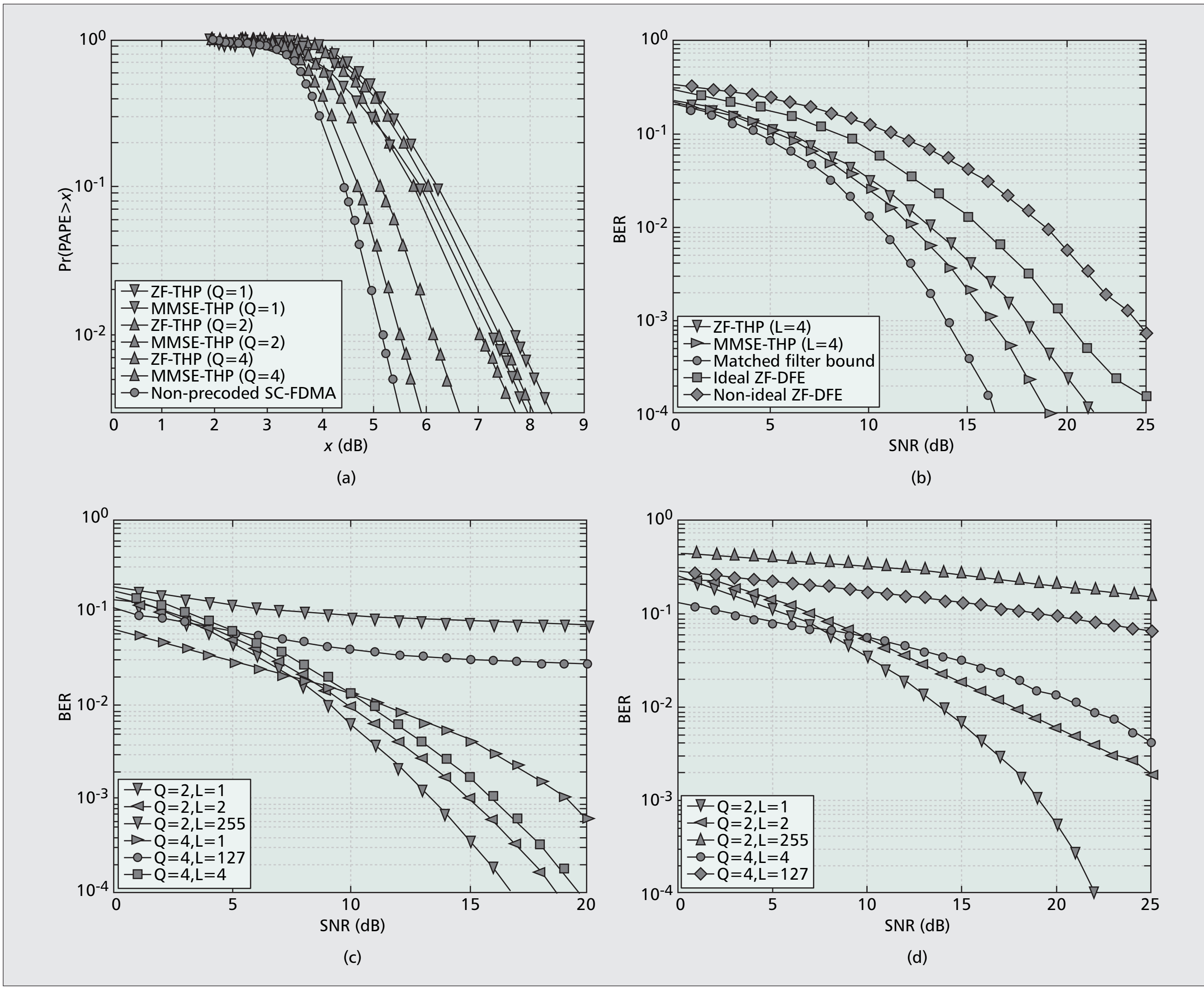

Figure 4. *BER performance and PAPR characteristics of precoded SC-FDMA: a) PAPR characteristics of the precoded SC-FDMA waveform; b) uncoded BER performance of ZF for SC-FDMA vs. MMSE DFE for* Q = 4 *blocks; c) uncoded BER performance of an SC-FDMA system with different blocks and MMSE THP; d) uncoded BER performance of an SC-FDMA system with different blocks and ZF-THP.*

BER Performance

Figure 4b shows the BER performance of ZF and MMSE-THP compared to the ideal and nonideal DFE for uncoded QPSK with four resource blocks. Both ZF and MSME THP outperform the ideal (i.e., assuming perfect feedback decisions) and nonideal DFE. MMSE-THP offers better BER performance than ZF-THP since MMSE-THP reduces the magnitude of the error resulting from the residual ISI (as a result of the combined channel and FDE) and the filtered additive noise, while the ZF-THP only cancels the residual ISI.

Figures 4c and 4d show the BER performance of MMSE and ZF pre-DFT THP, respectively, for different lengths of the precoder filter and different values of Q. From both figures, it can be seen that MMSE-THP outperforms ZF-THP. In addition, increasing the length of the precoder improves the performance for small values of L and degrades the performance. The performance improvement for small values of L is due to the fact that increasing L permits the precoder to cancel more ISI, but results in more noise amplification. As the length of the precoder is further increased, the precoder's gain γ increases, and as a result, when the receiver adjusts for the precoder's gain, noise amplification occurs.

Extension to MIMO

Although the 3GPP LTE standard only adopts MIMO transmission on the downlink, MIMO can be used in conjunction with SC-FDMA for uplink transmissions. In fact, MIMO is included in advanced LTE. MIMO takes advantage of the spatial separation between antenna elements to create uncorrelated spatial channels and exploit higher levels of spatial diversity. This translates to improved spectral and power efficiency. This will improve system capacity and overcome the power limitations of these systems. MIMO can be divided into three main categories:

• **Precoding** requires the same signal to be emitted from each of the transmit antennas with appropriate phase and gain weighting such that

If the channel information is available at the transmitter, it is possible to overcome the error propagation problem in the DFE through precoding. This achieves the ideal-DFE performance for coded and uncoded systems, and achieves high system throughput.

the signal power is maximized at the receiver input. This increases the signal gain from constructive combining. In [10] a study of the PAPR characteristics of beamforming with unitary precoding for SC-FDMA has shown that the increase in PAPR of the precoded waveform is not significant when compared to the single antenna system or the non-precoded MIMO SC-FDMA case. In addition, amplitude clipping can be used in order to maintain the PAPR below a certain level at the expense of performance degradation.

- **Spatial multiplexing** (**SM**) aims to increase the capacity of the system for the same bandwidth without any increase in transmit power.
- **Space time coding** (**STC**) aims to increase the diversity order of the system. In the context of SC-FDMA, [11] shows the possibility of employing transmit diversity for SC-FDMA in the form of space-time/frequency block coding (STBC/SFBC) or the more novel SC-SFBC. In [12] a study of the PAPR characteristics together with the error performance of MIMO SC-FDMA was presented for both SM and STC. It was shown that the PAPR and error performance are highly influenced by the choice of subcarrier mapping and vary from one MIMO scheme to the other. It was also shown that pulse shaping can be used to reduce the high PAPR of MIMO SC-FDMA, resulting in a performance degradation for both SM and STC.

In [13] Zhu and Letaief proposed the use of THP with FDE for single carrier MIMO systems. They introduced two schemes for parallel and successive precoding of data streams, and reported a significant improvement in the performance of MIMO systems compared to a conventional FDE. As demonstrated in this article, the computational complexity of the proposed frequency domain THP (FD-THP) is lower than that of the conventional time domain THP (TD-THP), which in turn grows as the number of transmit antennas increases. This indicates that FD-THP can be extended to MIMO without a significant increase in system complexity.

Conclusions and Future Work

SC-FDMA has been employed in the 3GPP LTE standard as the uplink transmission scheme because of its low PAPR characteristics compared to OFDMA. As a result SC-FDMA achieves more power-efficient transmission. In order to combat the detrimental effects of multipath fading channels, a common assumption is to employ FDE. FDE is a very attractive signal processing technique to deal with large time dispersive multipath channels, and can be implemented in the form of an FD-LE or FD-DFE. Although the FD-DFE offers a performance superior to that of conventional FD-LE, this technique suffers from performance degradation as a result of error propagation due to incorrect decisions, especially for long delay spread channels and coded systems. If the channel information is available at the transmitter, it is possible to overcome the error propagation problem in the DFE through precoding. This achieves the ideal DFE performance for coded and uncoded systems, and achieves high system throughput.

In this article we have presented the possibility of employing frequency domain transmit precoding for uplink SC-FDMA transmissions. There are two issues to be considered in the precoder design. First, because the implementation of transmit precoding requires perfect knowledge of the uplink channel with no latency, further work needs to address how channel estimation and tracking can assist the precoder in the case of mobility, channel estimation errors, and channel mismatch. Second, because the PAPR of the precoder's output is dependent on the channel fading, it is essential to employ some form of PAPR reduction.

References

[1] R. van Nee and R. Prasad, *OFDM for Wireless Multimedia Communications*, Artech House, 2000.

[2] H. G. Myung, *Single Carrier Orthogonal Multiple Access Technique for Broadband Wireless Communication*, Ph.D. thesis, Polytechnic Univ., Jan. 2007.

[3] T. Jiang and Y. Wu, "An Overview: Peak-to-Average Power Ratio Reduction Techniques for OFDM Signals," *IEEE Trans. Broadcasting*, vol. 54, June 2008.

[4] S. B. Slimane, "Reducing the Peak-to-Average Power Ratio of OFDM Signals through Precoding," *IEEE Trans. Vehic. Tech*., vol. 56, no. 2, Mar. 2007, pp. 686–95.

[5] D. Falconer *et al*., "Frequency Domain Equalization for Single-Carrier Broadband Wireless Systems," *IEEE Commun. Mag*., Apr. 2002.

[6] G. Huang, A. Nix, and S. Armour, "Decision Feedback Equalization in SC-FDMA," *IEEE 19th PIMRC*, Sept. 2008.

[7] M. Tomlinson, "New Automatic Equalizer Employing Modulo Arithmetic," *Elect. Lett.*, vol. 7, Mar. 1971, pp. 138–39.

[8] H. Harashima and H. Miyakawa, "Matched-Transmission Technique for Channels with Intersymbol Interference," *IEEE Trans. Commun*., vol. 20, Aug. 1972, pp. 774–80.

[9] N. Benvenuto and S. Tomasin, "On the Comparison between OFDM and Single-Carrier Modulation with a DFE Using a Frequency-Domain Feedforward Filter," *IEEE Trans. Commun*., vol. 50, no. 6, June 2002, pp. 947–55.

[10] H. G. Myung *et al*., "Peak Power Characteristics of Single Carrier FDMA MIMO Precoding System," *IEEE VTC 2007-Fall*, Baltimore, MD, Oct. 2007.

[11] C. Ciochina *et al*., "A Novel Space-Frequency Coding Scheme for Single-Carrier Modulations," *Proc. IEEE PIMRC*, Athens, Greece, Sept. 2007.

[12] N. Tavangaran, A. Wilzeck, and T. Kaiser, "MIMO SC-FDMA System Performance for Space Time/Frequency Coding and Spatial Multiplexing," *Int'l. ITG Wksp. Smart Antennas*, 2008, pp. 382–86.

[13] Z. Yu and K. B. Letaief, "Frequency Domain Equalization with Tomlinson-Harashima Precoding for Single Carrier Broadband MIMO Systems," *IEEE Trans. Wireless Commun*., vol. 6, no. 12, Dec. 2008, pp. 4420–31.

Biographies

MOHAMED B. NOUNE (Mohamed.Noune@bristol.ac.uk) received his B.Eng. and M.Sc. in communications systems and signal processing from the University of Bristol, United Kingdom, in 2004 and 2006, respectively. He then joined the Centre for Communications Research (CCR) of the University of Bristol pursuing a Ph.D. degree in the area of transmitter and receiver optimization for future generation systems. He is the recipient of several awards, including the Gold Medal in the National Contest of Mathematics in 2000, the Algerian President's award for outstanding performance in the Baccalauréat exam in 2000, and the IEEE UK and NI best Communications Chapter award in 2005. His research interests include space-time coding and MIMO communications systems, OFDM and OFDMA systems, multiuser diversity and resource allocation, and broadband wireless communications.

ANDREW R. NIX (Andy.Nix@bristol.ac.uk) received B.Eng. and Ph.D. degrees from the University of Bristol in 1989 and 1993, respectively. He is currently a professor of wireless communication systems with the University of Bristol. He has managed numerous European Union, Engineering and Physical Sciences Research Council, and Department of Trade and Industry funded projects. He is the author or coauthor of more than 250 papers published in international journals and conference proceedings. His main research interests include broadband wireless communications, radiowave propagation modeling, cellular network optimization, and advanced digital modulation/reception techniques.